

# A role for endothelial cells in promoting the maturation of astrocytes through the apelin/APJ system in mice

メタデータ	言語: eng 出版者: 公開日: 2021-07-05 キーワード (Ja): キーワード (En): 作成者: メールアドレス: 所属:
URL	<a href="https://doi.org/10.24517/00062992">https://doi.org/10.24517/00062992</a>

This work is licensed under a Creative Commons Attribution-NonCommercial-ShareAlike 3.0 International License.



# A role for endothelial cells in promoting the maturation of astrocytes through the apelin/APJ system in mice

Susumu Sakimoto<sup>1,2</sup>, Hiroyasu Kidoya<sup>1</sup>, Hisamichi Naito<sup>1</sup>, Motohiro Kamei<sup>2</sup>, Hirokazu Sakaguchi<sup>2</sup>, Nobuhito Goda<sup>4</sup>, Akiyoshi Fukamizu<sup>3</sup>, Kohji Nishida<sup>2</sup> and Nobuyuki Takakura<sup>1,5,\*</sup>

## SUMMARY

Interactions between astrocytes and endothelial cells (ECs) are crucial for retinal vascular formation. Astrocytes induce migration and proliferation of ECs via their production of vascular endothelial growth factor (VEGF) and, conversely, ECs induce maturation of astrocytes possibly by the secretion of leukemia inhibitory factor (LIF). Together with the maturation of astrocytes, this finalizes angiogenesis. Thus far, the mechanisms triggering LIF production in ECs are unclear. Here we show that apelin, a ligand for the endothelial receptor APJ, induces maturation of astrocytes mediated by the production of LIF from ECs. *APJ* (*Aplnr*)- and *Apln*-deficient mice show delayed angiogenesis; however, aberrant overgrowth of endothelial networks with immature astrocyte overgrowth was induced. When ECs were stimulated with apelin, LIF expression was upregulated and intraocular injection of LIF into *APJ*-deficient mice suppressed EC and astrocyte overgrowth. These data suggest an involvement of apelin/APJ in the maturation process of retinal angiogenesis.

**KEY WORDS:** Astrocytes, Endothelial cells, Apelin, Mouse

## INTRODUCTION

The retina is composed of several cell types. Interactions between endothelial cells (ECs), astrocytes and neuronal cells is crucial for fine capillary network formation by ECs. Before the onset of interactions between ECs and astrocytes in the retina of postnatal mice, astrocytes invade from the optic nerve head via the axons of retinal ganglion cells. Controlling this association between different cell components, platelet-derived growth factor A (PDGFA) from retinal ganglion cells promotes growth of immature astrocytes expressing PDGF receptor  $\alpha$  (PDGFR $\alpha$ ). This results in astrocyte network formation (Fruttiger et al., 1996). Subsequently, ECs from the optic nerve head invade and migrate over the network-forming astrocytes as a template. A crucial role of vascular endothelial growth factor (VEGF), produced by astrocytes, in guiding endothelial tip cells in the vascular branch and in the proliferation of endothelial stalk cells behind the tip cells has been reported (Gerhardt et al., 2003).

In the course of retinal angiogenesis, astrocytes act as proangiogenic accessory cells, as described above; however, upon becoming overlaid with ECs, it has been suggested that their proangiogenic activity ceases and they instead stabilize newly developed blood vessels (West et al., 2005; Kubota et al., 2008). Anatomical analysis has revealed that astrocytes expressing low levels of glial fibrillary acidic protein (GFAP) firstly invade the retina, gradually express higher levels of GFAP, and become quiescent (Chu et al., 2001; Gariano, 2003). Therefore, it has been

suggested that ECs might change astrocyte characteristics (Zhang and Stone, 1997), with several lines of evidence suggesting that leukemia inhibitory factor (LIF) derived from ECs is a direct maturation factor for immature astrocytes in vitro (Mi et al., 2001) and in vivo (Kubota et al., 2008). However, the mechanism responsible for controlling LIF production by ECs for maturation of astrocytes has not been elucidated.

During the process of angiogenesis, maturation of blood vessels is induced by angiopoietin 1 (ANG1; also known as ANGPT1), a ligand for endothelial receptor tyrosine kinase TIE2 (also known as TEK), produced by mural cells, which directly adhere to ECs. This results in structural stabilization of the blood vessels (Sato et al., 1995; Suri et al., 1996; Augustin et al., 2009). Apelin is a ligand for the G protein-coupled receptor APJ expressed on ECs. We previously reported that activation of TIE2 promotes apelin production from ECs and that ANG1/TIE2-mediated maturation of blood vessels, such as their enlargement and non-leaky blood vessel formation, is partly dependent on APJ activation by apelin ligation (Kidoya et al., 2008; Kidoya et al., 2010). Recently, involvement of the apelin/APJ system in retinal angiogenesis has been reported (Kasai et al., 2008; del Toro et al., 2010) in which delayed angiogenesis and reduced proliferation of stalk cells was observed in gene ablation analysis of apelin (*Apln*) and apelin receptor (*APJ*; *Aplnr* – Mouse Genome Informatics) (Kasai et al., 2008; del Toro et al., 2010; Kidoya et al., 2010). In contrast to the constitutive expression of TIE2, as well as of VEGF receptor 2 (VEGFR2; also known as FLK1 and KDR), APJ expression in ECs is transient. From the onset of retinal angiogenesis, most network-forming ECs express APJ until postnatal day (P) 7; however, after reaching the marginal zone of the retina, ECs stop expressing APJ at P12, except for the larger veins (Saint-Geniez et al., 2003). Taken together, these findings imply that apelin/APJ acts as a maturation factor for newly developed blood vessels, in addition to its proangiogenic function.

During retinal angiogenesis, it is suggested that ECs and astrocytes mature simultaneously in a mutually dependent manner. However, whether maturation arrest of blood vessels affects

<sup>1</sup>Department of Signal Transduction, Research Institute for Microbial Diseases, Osaka University, 3-1 Yamada-oka, Suita, Osaka 565-0871, Japan. <sup>2</sup>Department of Ophthalmology, Osaka University Graduate School of Medicine, Suita, Osaka 565-0871, Japan. <sup>3</sup>Center for Tsukuba Advanced Research Alliance, Institute of Applied Biochemistry, University of Tsukuba, Ibaraki 305-8577, Japan. <sup>4</sup>Department of Life Science and Medical Bio-Science, School of Advanced Science and Engineering, Waseda University, 2-2 Wakamatsu-cho, Shinjuku-ku, Tokyo 162-8480, Japan. <sup>5</sup>JST, CREST, K's Gobancho, 7 Gobancho, Chiyoda-ku, Tokyo 102-0076, Japan.

\* Author for correspondence (ntakaku@biken.osaka-u.ac.jp)

astrocyte maturation is not yet clear. Because apelin/APJ is mainly involved in the maturation of blood vessels, we used mice with *Apln* as well as *APJ* mutations to ask whether the maturation of astrocytes is affected by a deficiency of apelin or APJ. Moreover, we investigated how astrocyte maturation conversely affects the growth of ECs in order to understand mutual EC/astrocyte regulation.

## MATERIALS AND METHODS

### Mice

All experiments were carried out under the guidelines of the Osaka University Committee for Animal Research. C57BL/6 (Japan SLC, Shizuoka, Japan), *APJ* knockout (KO) (Ishida et al., 2004) and *Apln* KO (Kidoya et al., 2008) mice were used in these studies. Animals were housed in environmentally controlled rooms of the animal experimentation facility at Osaka University.

### Quantitative reverse transcription real-time PCR (qRT-PCR)

Total RNA was extracted from cells and tissues using the RNeasy Plus Mini Kit (Qiagen) and transcribed into cDNA using the ExScript RT Reagent Kit (Takara) according to the manufacturers' protocols. Real-time PCR analysis was performed using Platinum SYBR Green qPCR SuperMix-UDG (Invitrogen) and an Mx3000P QPCR System (Stratagene). The baseline and threshold were adjusted according to the manufacturer's instructions. PCR was performed on cDNA using the primers listed in supplementary material Table S1. The level of expression of the target gene was normalized to that of *Gapdh* in each sample.

### Tissue immunostaining and in situ hybridization (ISH)

Tissue preparation and staining were as previously reported (Takakura et al., 2000). Eucleated eyes were fixed in 4% paraformaldehyde. Antibodies for staining were anti-PECAM1 (BD Biosciences, 1:100; or Chemicon International, 1:100), anti-GFAP (Sigma-Aldrich, 1:100), anti-PDGFR $\alpha$  (eBioscience, 1:100), anti-desmin (DAKO, 1:100), anti-PAX2 (Covance, 1:100), anti-KI67 (DAKO, 1:100), anti-neurofilament (American Research Products, 1:100), anti-type IV collagen (Cosmo Bio, 1:100), anti-HIF1 $\alpha$  (1:100) (Kurihara et al., 2010), anti-apelin (1:100) (Kidoya et al., 2008) and anti-APJ (1:100) (Kidoya et al., 2008). The secondary antibodies used were Alexa Fluor 488/546/647-conjugated IgGs (Invitrogen, 1:200) or FITC/Cy5-conjugated IgGs (Jackson ImmunoResearch Laboratories, 1:200).

For whole-mount ISH, retinas were briefly digested with proteinase K and hybridized with digoxigenin-labeled antisense RNA probes.

For determination of hypoxic tissue, mice were injected intraperitoneally with 60 mg/kg body weight Hypoxyprobe-1 (pimonidazole hydrochloride) (Natural Pharmacia International) before harvesting retinas for tissue processing and staining according to the manufacturer's instructions. Six animals per group were analyzed. A total of eight straight lines were drawn in each retina: four from the optic nerve to the vascular front representing a vascularized area; and four from the vascular front to the peripheral retina as an avascular area. Samples were visualized using conventional microscopy (with a DM5500B equipped with HCX PL FLVOTAR 5/0.15 and HCX PL FLVOTAR 0/0.15 dry objective lenses, Leica) or confocal microscopy (TCS/SP5 equipped with HC PLAN APO 2/0.70 and HCXPL APO 4/1.25-0.75 oil objective lenses, Leica) at room temperature. Images were acquired with a DFC 500 digital camera (Leica) and processed with the Leica application suite and Adobe Photoshop CS3 software. All images shown are representative of three to six independent experiments.

### Retina quantification

Complete high-resolution three-dimensional (3D) rendering of whole-mount retinas was achieved using the confocal microscope described above. The cells of interest (PAX2<sup>+</sup> astrocytes, PAX2<sup>+</sup> KI67<sup>+</sup> astrocytes and HIF1 $\alpha$ <sup>+</sup> cells) were manually scored in six random 350 $\times$ 350  $\mu$ m or 250 $\times$ 250  $\mu$ m (HIF1 $\alpha$ <sup>+</sup> cells) fields of view (FOV) per retina photographed at 40 $\times$  or 63 $\times$  magnification using the software of the Leica application suite. To determine cell number and measure the capillary density of the retinas, six animals per group were analyzed. After conversion to 8-bit

grayscale using ImageJ software, the capillary density in the vascularized area was quantified from the pixels. The vascularized areas were defined as the region near the vascular front without the regions from the very tips to the first vascular loop. The avascular areas were defined as the regions ~500  $\mu$ m ahead of the vascular front. HIF1 $\alpha$ <sup>+</sup> cells were counted in different areas.

### Flow cytometry analysis

Retinas of at least five WT and *APJ* KO mouse neonates were incubated for 30 minutes at 37°C in DMEM containing 1% collagenase (Wako, Osaka, Japan) before cells were dissociated by gentle trituration. Cells were pretreated with Fc-Blocker (BD Biosciences Pharmingen) and stained with FITC-conjugated anti-CD140a (PDGFR $\alpha$ ) monoclonal antibody and phycoerythrin-conjugated anti-CD31 monoclonal antibody (BD Biosciences Pharmingen). Procedures for cell preparation and staining were as previously reported (Kidoya et al., 2008). The stained cells were analyzed and sorted using a FACSARIA flow cytometer (BD) with FlowJo (TreeStar) or CellQuest (BD) software. Dead cells were excluded from the analyses using the 2D profile of forward versus side scatter. Using these negative and positive control tubes, we set fluorescence voltages and the compensation matrix according to the instructions of the manufacturer. We applied these setting parameters to all samples analyzed.

### Intraocular injection

Sterile PBS with or without 1 mg/ml apelin (Bachem), 0.5 mg/ml LIF (ESGRO, Chemicon) or 1 mg/ml sFLT1 was injected into the vitreous humor of P3 mice using a sterile injection capillary with an automatic microinjector (FemtoJet, Eppendorf). Mice were sacrificed 48 hours later and the retinas isolated for cell purification or immunohistochemistry.

### Cell culture

The mouse microvascular endothelial cell line bEnd.3 or HUVECs were cultured in six-well plates for 12 hours in DMEM or Humedia EG2 (Kurabo, Osaka, Japan), respectively. Cells were then incubated in medium supplemented with 1% fetal bovine serum (FBS). After 6 hours of serum deprivation, cells were stimulated with basal medium containing 20 ng/ml VEGFA 165 (PeproTech) for 18 hours and subsequently incubated with 50 or 500 ng/ml apelin. Culturing of retinal cells was performed as described previously (West et al., 2005). P1 WT retinas were dissected as indicated above, redissociated in DMEM containing 10% FBS and then plated on poly-D-lysine-coated coverslips in 24-well plates at 1.5 $\times$ 10<sup>6</sup> cells/well and incubated at 37°C, 5% CO<sub>2</sub> for 24 hours. Retinal cells were incubated for 24 hours with supernatant of bEnd.3 cells that had been treated with apelin for 24 hours.

### Statistical analysis

Data are presented as mean $\pm$ s.d. for the in vitro studies and mean $\pm$ s.e. for in vivo studies. For statistical analysis, the Statcel 2 software package (OMS) was used with analysis of variance performed on all data followed by Tukey-Kramer multiple comparison testing. When only two groups were compared, a two-sided Student's *t*-test was used. *P*<0.05 was considered statistically significant.

## RESULTS

### Dense astrocyte network formation is induced in APJ-deficient mice

Because it has been reported that *APJ* mutant mice show retarded endothelial network formation in the retina (del Toro et al., 2010), we first investigated the development of, and network formation by, astrocytes from P0 to P7 (Fig. 1A). Using anti-PDGFR $\alpha$  antibody in immunohistochemistry (IHC) to identify these cells, we found that astrocyte network formation was similar in wild-type (WT) and *APJ* KO mice at P1; however, a dense network appeared in *APJ* KO mice at P5 and continued at least until P7. PDGFR $\alpha$ <sup>+</sup> astrocytes were also analyzed by flow cytometry and their number calculated as a proportion of the total number of retinal cells at P5. A significantly greater proportion of astrocytes was found to be present in *APJ* KO

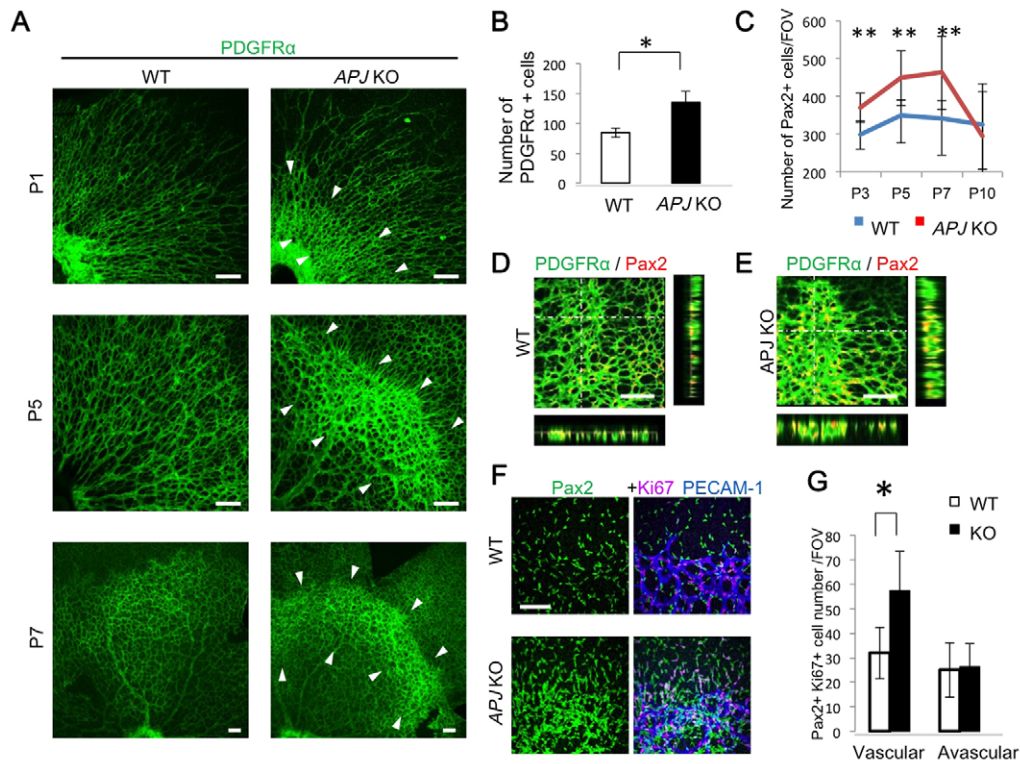


**Fig. 1. APJ KO mice show irregular remodeling and proliferation of retinal astrocytes.** (A) Immunohistochemistry (IHC) for PDGFR $\alpha$  (green) in the P1, P5 and P7 developing retina of wild-type (WT) or APJ KO mice. Note the dense astrocyte network (surrounded by arrowheads) in APJ KO mice. (B) Quantitative evaluation of the number of PDGFR $\alpha$ <sup>+</sup> cells per  $5 \times 10^4$  cells analyzed by FACS. Dissociated retinal cells from P5 WT or APJ KO mice were used ( $n=4$ ,  $*P<0.05$ ). (C) Transition of the number of astrocytes identified as PAX2<sup>+</sup> nuclei in vascularized areas. Data are the mean of six random fields of view (FOV) in the vascularized area per retina ( $n=6$ ,  $**P<0.01$ ). (D,E) Confocal microscopy images of PDGFR $\alpha$ <sup>+</sup> (green) and PAX2<sup>+</sup> (red) astrocytes in WT (D) and APJ KO (E) P5 retinas. z-stack images show two-layered astrocytes in APJ KO retina. (F) Proliferation status of astrocytes in P5 retinas from WT and APJ KO mice. Retinas were stained with antibodies against PAX2 (green), KI67 (magenta) and PECAM1 (blue). Note the marked proliferation of PAX2<sup>+</sup> KI67<sup>+</sup> astrocytes (white or light blue) in vascular areas of APJ KO mice. (G) Quantification of PAX2<sup>+</sup> KI67<sup>+</sup> astrocytes in the vascularized or non-vascularized retinal areas. Six random FOV were examined per retina ( $n=6$ ,  $*P<0.05$ ). Error bars indicate s.d. Scale bars: 100  $\mu$ m.

than WT mice (Fig. 1B). We next calculated the number of astrocytes expressing PAX2, a nuclear transcription factor present in all cells of the astrocyte lineage (Fig. 1C-E). Although the number of PAX2<sup>+</sup> astrocytes in APJ KO mice was higher than in WT mice from P3 to P7, it gradually decreased to WT levels, suggesting negative-feedback regulation (Fig. 1C). z-stack images suggested that a thicker retinal astrocyte layer was induced in APJ KO than in WT mice owing to the generation of two layers of astrocytes at P5 (Fig. 1D,E). Next, we stained the retina for the EC marker PECAM1 (CD31) and with anti-PAX2 antibody, as well as for the cell proliferation marker (KI67). High-density areas of PAX2<sup>+</sup> KI67<sup>+</sup> proliferating astrocytes were present in vascular but not avascular areas (Fig. 1F,G), suggesting that astrocyte proliferation is associated with ECs.

Next we assessed the degree of astrocyte maturation in APJ KO mice. In WT mice, astrocytes that are initially weakly GFAP positive start to express a high level of GFAP at P5 (Fig. 2A-C). The strongly GFAP-positive astrocytes present from the optic nerve head up to the beginning of the dense astrocyte sheet area did not differ substantially between APJ KO and WT mice. However, within the dense astrocyte sheet there were fewer strongly GFAP-positive astrocytes in the APJ KO mice (Fig. 2A,D,E). Consistent with this, levels of *Gfap* mRNA were reduced in APJ KO mice at all periods examined (Fig. 2F). Comparing other astrocyte differentiation markers in APJ KO and WT mice revealed similar levels of

expression for the lineage markers vimentin (*Vim*) and *Pax2* but a significant reduction in the mature astrocyte markers *S100b* and *Gfap* in the knockouts (Fig. 2G). These data suggest that APJ deficiency does not affect the development of astrocytes but influences their maturation.

### APJ deficiency indirectly induces dense endothelial sheets via overgrowth of immature astrocytes

It has been reported that both APJ KO and *Apln* KO mice show delayed retinal angiogenesis (Kasai et al., 2008; del Toro et al., 2010). However, as we found aberrant overgrowth of immature astrocytes in APJ KO mice, we hypothesized that abnormal overgrowth during blood vessel formation should also be induced in APJ KO mice indirectly owing to the defect of APJ in ECs, as weakly GFAP-positive astrocytes possess proangiogenic properties. Although retinal vessel outgrowth from the optic nerve head was indeed impaired in APJ KO mice (supplementary material Fig. S1) as previously reported (del Toro et al., 2010), a dense endothelial network-forming area was frequently observed at the migrating front of the retinal vasculature after P5 (Fig. 3A-C).

Consistent with hyperproliferation of ECs in APJ KO mice, the retinas of these mice were found by in situ hybridization (ISH) to express more *Vegfa* mRNA in the peripheral region of

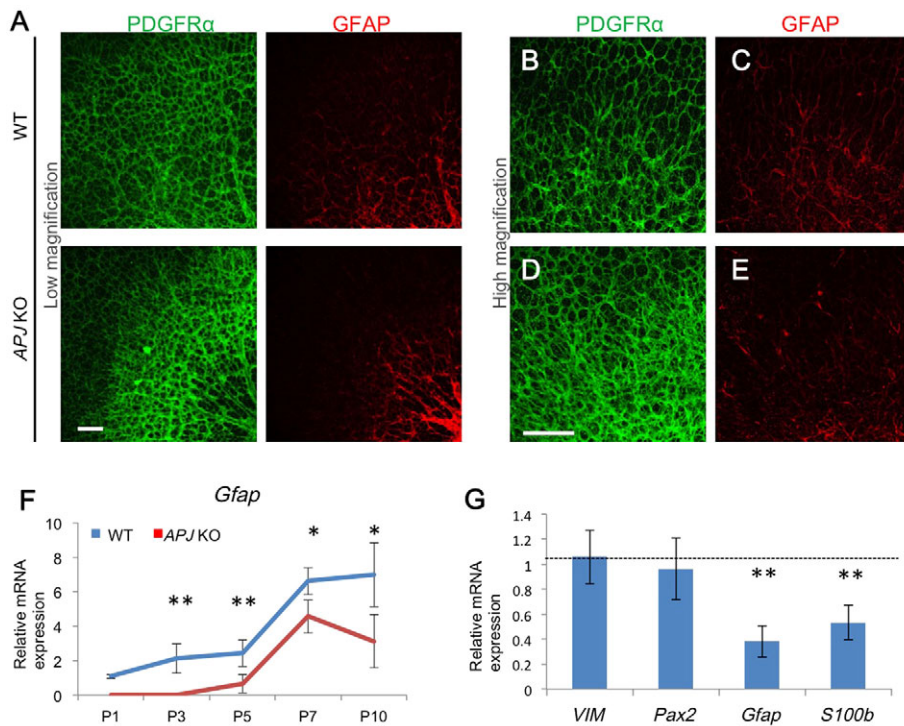


**Fig. 2. Suppression of astrocyte maturation in *APJ* KO developing retina.** (A) Retinal astrocytes stained for PDGFR $\alpha$  (green) and GFAP (red) in P5 WT and *APJ* KO mice. (B-E) High-magnification views of retinal astrocytes around the migrating front of the vascular network area as shown in Fig. 1F. Note the weak positivity for GFAP in overgrown astrocytes in *APJ* KO mice. (F) Quantitative RT-PCR (qPCR) analysis of *Gfap* expression using isolated RNA from FACS-sorted PDGFR $\alpha^+$  cells at various retinal stages ( $n=3$ ,  $*P<0.05$ ,  $**P<0.01$ ). (G) qPCR analysis of retinal astrocyte marker expression with RNA isolated from sorted PDGFR $\alpha^+$  cells of P5 retina. Data represent relative mRNA expression from *APJ* KO mice as compared with WT mice set as unity ( $n=3$ ,  $**P<0.01$ ). Dotted line indicates level of WT. Error bars indicate s.d. Scale bars: 100  $\mu$ m.

the endothelial network-forming area than did WT mice at P5 (Fig. 3D). Moreover, comparing sorted retinal PDGFR $\alpha^+$  astrocytes revealed greater *Vegfa* mRNA expression in *APJ* KO than in WT mice (Fig. 3E). VEGF expression is known to be regulated by hypoxia via hypoxia inducible factor 1 $\alpha$  (HIF1 $\alpha$ ). It has been reported that suppression of retinal vascular growth by VEGF-Trap injections primarily leads to VEGF upregulation, GFAP downregulation, and dense network formation in retinal astrocytes (Uemura et al., 2006). Moreover, West et al. have clearly demonstrated that hypoxia inhibits the maturation of astrocytes, resulting in VEGF upregulation, using models for retinopathy of prematurity (West et al., 2005). Currently, it is

widely accepted that hypoxia is crucial for the regulation of astrocyte maturation. Therefore, it is possible that the hyperproliferation of ECs observed in *APJ* KO mice is caused by hypoxia induced by impaired vessel outgrowth. Indeed, compared with WT mice, slightly stronger Hypoxyprobe-1 signals were observed in the avascular area of the vascular front (asterisks in Fig. 4A,B) and the hypovascular areas in the middle of the vascular network (the areas enclosed by the dashed lines in Fig. 4A) in *APJ* KO mice. Although the levels of *Hif1a* mRNA were not significantly different in the whole retinas of WT and *APJ* KO mice (supplementary material Fig. S3), nuclear translocation of HIF1 $\alpha$ , indicating its state of activation, was

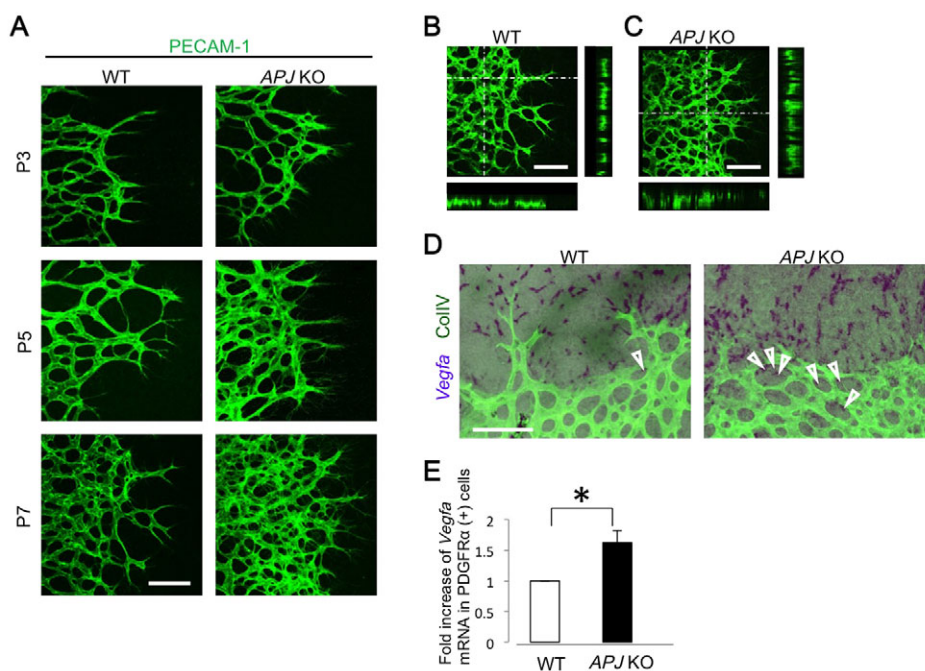


**Fig. 3. Aberrant overgrowth of ECs in *APJ* KO mice.** (A) Whole-mount anti-PECAM1 immunostaining of the developing front of P3, P5 and P7 WT and *APJ* KO mice. (B,C) Confocal microscopy images of PECAM1 $^+$  ECs in P7 WT (B) and *APJ* KO (C) mouse retinas. z-stack images show a denser EC layer in *APJ* KO than in WT retina. (D) In situ hybridization (ISH) for *Vegfa* combined with IHC for collagen IV in the vascular front. Note the increase of *Vegfa* mRNA in *APJ* KO retina. Arrowheads indicate upregulation of *Vegfa* mRNA even in the vascular area. (E) qPCR analysis of *Vegfa* mRNA expression in retinal PDGFR $\alpha^+$  astrocytes from P5 retinas of WT and *APJ* KO mice ( $n=3$ ,  $*P<0.05$ ). Error bars indicate s.d. Scale bars: 100  $\mu$ m.

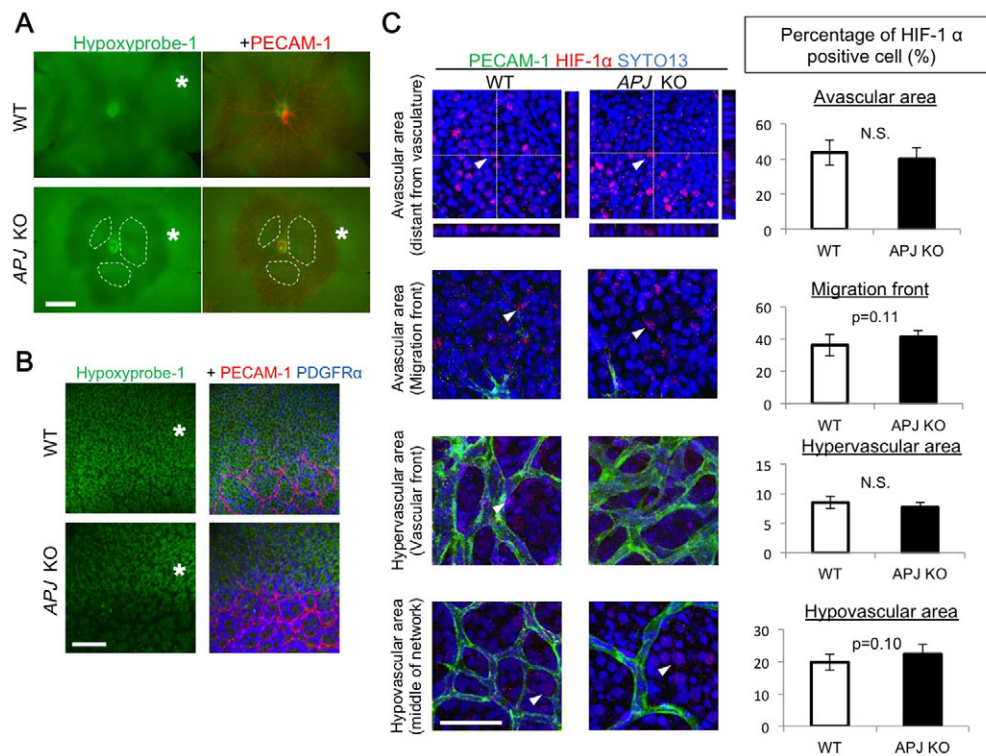


**Fig. 4. Evaluation of hypoxic status in *APJ* KO mice.** (A) Low-magnification images of hypoxic status in *APJ* KO mouse retina. Detection of PECAM1 (red) and Hypoxyprobe-1 (green) in P5 WT and *APJ* KO retinas. Asterisks indicate avascular areas of the vascular front and the areas demarcated by dashed lines indicate the hypovascular areas in the middle of the vascular network. (B) Higher magnification images of hypoxic status showing PECAM1 (red), PDGFR $\alpha$  (blue) and Hypoxyprobe-1 (green) in P5 WT and *APJ* KO retinas. (C) Nuclear translocation of HIF1 $\alpha$  protein in *APJ* KO mice. Retinas of WT and *APJ* KO mice were dissected at P5 and whole-mount immunostaining was performed using anti-PECAM1 (green) and anti-HIF1 $\alpha$  (red) antibodies and analyzed in different areas. Arrowheads indicate nuclear positivity for HIF1 $\alpha$ . z-stack image showing localization of HIF1 $\alpha$  in nuclei stained with SYTO13 (blue). (Right) Percentages of nuclear HIF1 $\alpha$ <sup>+</sup> cells in the areas described were quantitatively evaluated. Four random FOV in the vascularized area were examined per retina ( $n=6$ ). N.S., not significant. Error bars indicate s.d. Scale bars: 500  $\mu$ m in A; 100  $\mu$ m in B; 50  $\mu$ m in C.

slightly enhanced in areas where more intense Hypoxyprobe-1 signals were observed in the *APJ* KO mice (Fig. 4C). However, the difference in HIF $\alpha$  nuclear translocation in WT and *APJ* KO mice was not statistically significant.

These data suggest that the VEGFA overexpression observed in astrocytes from *APJ* KO mice and the partial dense vascular network formation are dependent on hypoxia as a primary effect of APJ deficiency. However, compared with other models using VEGF-Trap (Uemura et al., 2006) or retinopathy of prematurity (West et al., 2005), in which blood vessel formation in the retina is completely abolished and strong hypoxia is induced, the degree of vascular defects and hypoxia observed here in *APJ* KO mice was not severe. Therefore, we consider that not only hypoxia but also other mechanisms underlie the maturation of astrocytes affected by APJ.

It is possible that APJ is expressed on astrocytes and that this, rather than its absence from ECs, affects the growth of immature astrocytes directly. However, we were unable to detect APJ expression on PDGFR $\alpha$ <sup>+</sup> astrocytes, whereas it was present on ECs (supplementary material Fig. S2). Moreover, we assessed whether the overgrowth of astrocytes is affected by aberrant growth of retinal ganglion cells. As shown in Fig. 5A, radially migrated well-organized retinal ganglion cells were present in *APJ* KO mice to the same extent as in WT mice. Expression of *Pdgfra* mRNA in retinal tissue was not increased in *APJ* KO mice relative to WT mice (Fig. 5B).

Next, we tested whether moderate, but not severely, delayed angiogenesis in the retina, as observed in *APJ* KO mice, affects astrocyte proliferation in WT mice by neutralizing VEGF using injections of soluble (s) FLT1 (VEGFR1). We started to neutralize VEGF from P3 and assessed its effects on vascular formation at P5, as severe vascular defects were induced when VEGF was neutralized from P0, as previously reported (Uemura et al., 2006). As shown in Fig. 5C, treatment with sFLT1 according to this schedule retarded the outgrowth of blood vessels to a similar extent to that observed in *APJ* KO mice. Although a partial dense astrocyte sheet was observed (Fig. 5C, arrow), z-stack images suggested that the thickness of the astrocyte layer was almost the same in PBS-treated or sFLT1-treated mice (Fig. 5D). Furthermore, increases in the total number and proliferation of astrocytes were not observed (Fig. 5E-H). These data suggest that molecular cues that are absent owing to the lack of APJ in ECs affect overgrowth by immature astrocytes.

### Exogenous apelin induces the expression of GFAP in retinal astrocytes

Based on this result that a lack of APJ on ECs affects the outgrowth of immature astrocytes, we next examined whether apelin is involved in astrocyte differentiation and proliferation *in vivo*. Immunohistochemical analysis revealed that GFAP expression on astrocytes at P5 was enhanced following intraocular injection of apelin into WT mice at P3 (Fig. 6A). We confirmed upregulation

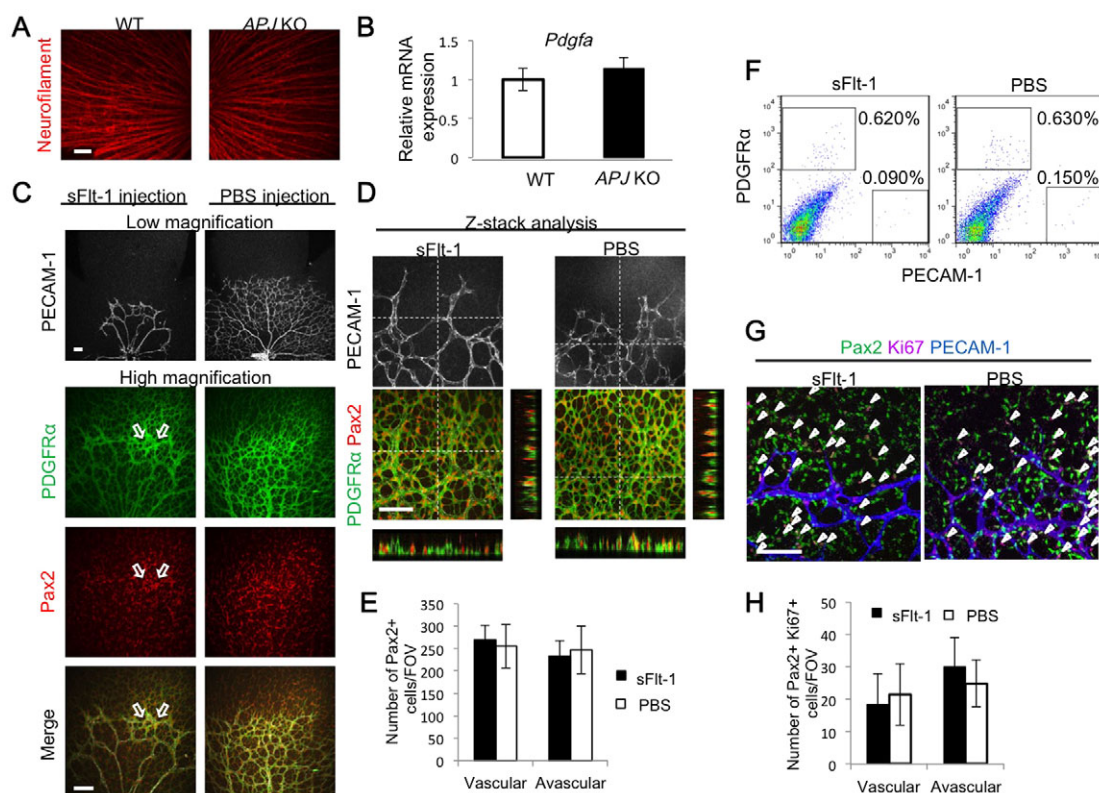


**Fig. 5. Evaluation of neuronal cell development in the absence of APJ and its effects on proliferation of astrocytes mediated by retardation of vascular development.** (A) The morphology of retinal ganglion cells in P3 WT and *APJ* KO mouse retinas. Retinas were stained with anti-neurofilament antibody. (B) qPCR analysis of *Pdgfa* mRNA expression in P5 WT and *APJ* KO retinas. (C–G) Effect of vascular retardation on astrocyte development in the retina assessed by intraocular injection of soluble (s) FLT1 or PBS (control). (C) Retinas were stained with antibodies against PDGFRα (green), PAX2 (red) and PECAM1 (white) at P5, 48 hours after treatment with sFLT1 or PBS. Although sFLT1 retarded vascular outgrowth, this degree of vascular defectiveness did not induce substantially abnormal networks of astrocytes at the vascular front with the exception of slight dense astrocyte network formation (arrows in C). (D) z-stack analysis showing no differences in the thickness of the glial cell layer or in the number of PAX2<sup>+</sup> cells between PBS- and sFLT1-treated mice. (E) Quantification of PAX2<sup>+</sup> astrocytes in the vascular and avascular areas. (F) Flow cytometry analysis of P5 retina from PBS- and sFLT1-treated mice ( $n=8$ ). The number of PECAM1<sup>+</sup> cells decreased with sFLT1 treatment but the number of PDGFRα<sup>+</sup> cells did not change. (G) Proliferation status of astrocytes in P5 retinas from PBS- and sFLT1-treated mice. Retinas were stained with antibodies against PAX2 (green), KI67 (magenta) and PECAM1 (blue). Arrowheads indicate PAX2<sup>+</sup> KI67<sup>+</sup> astrocytes in vascular areas of P5 retinas from PBS- and sFLT1-treated mice. (H) Quantification of PAX2<sup>+</sup> KI67<sup>+</sup> astrocytes in the vascularized and non-vascularized retinal areas. Four random FOV per retina were examined ( $n=5$ ). Error bars indicate s.d. Scale bars: 100 μm.

of *Gfap* mRNA in sorted PDGFRα<sup>+</sup> astrocytes from retinal tissues (Fig. 6B). Contrary to expectations, however, additional apelin in the WT retina did not alter blood vessel formation (Fig. 6A,C).

Next, we assessed whether apelin affected overgrowth by astrocytes in *Apln* KO mice. As in *APJ* KO mice, hyperproliferation of PDGFRα<sup>+</sup> PAX2<sup>+</sup> astrocytes was observed in *Apln* KO mice at P5 (Fig. 6D). Such astrocytes were weakly positive for GFAP (data not shown). Similar to the experiment shown in Fig. 6A, *Apln* KO mice at P3 were given intraocular injections of apelin and retinal gliogenesis was observed at P5. This demonstrated that apelin prevented the hyperproliferation of astrocytes that would otherwise result from the lack of apelin (Fig. 6D,E). Moreover, the capillary density in the migrating front of the vascular network was decreased in *Apln* KO mice injected intraocularly with apelin (Fig. 6D,F).

Because we failed to detect APJ expression in astrocytes, it is possible that ECs produce maturation factors for astrocytes when they are stimulated by apelin. We added supernatants from 24-hour apelin-stimulated cultures of cells of the bEnd3 EC line derived from mouse brain to primary cultures of retinal cells from WT mice at P1 (Fig. 7A). We did not detect a direct effect of apelin on the induction of GFAP expression by astrocytes, but these culture supernatants

enhanced its expression in retinal cells. Candidate factors for inducing GFAP positivity in astrocytes are LIF and ciliary neurotrophic factor (CNTF), which are both members of the IL6 family (Kishimoto et al., 1995). We investigated the expression of IL6 family cytokines in PECAM1<sup>+</sup> ECs directly sorted from the retina of *APJ* KO mice or WT mice at P5. We could not detect IL6, oncostatin M, cardiotrophin 1 or IL11 in ECs from WT or *APJ* KO mice, and CNTF expression was similar in ECs from both sources. By contrast, LIF expression was markedly lower in *APJ* KO than in WT mice (Fig. 7B). Transcription of *LIF* was upregulated transiently upon stimulation of human umbilical vein ECs (HUVECs) with apelin (Fig. 7C). These data suggest that stimulation of ECs by apelin induces production of LIF in an APJ-dependent manner, which then influences astrocyte maturation.

### Overgrowth of immature astrocytes resulting from a lack of APJ in ECs is abrogated by LIF injection

On the basis of the above results, we suggest that a lack of apelin/APJ system activity in ECs induces overgrowth of immature astrocytes followed by inhibition of their maturation,

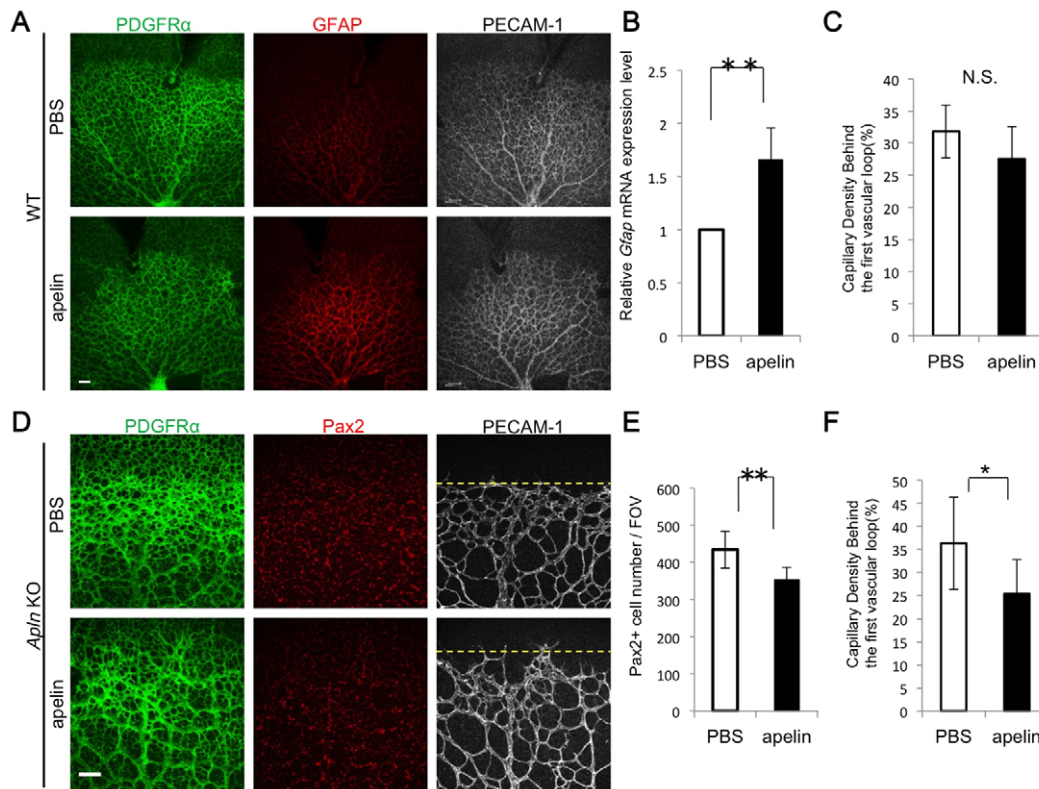


**Fig. 6. Exogenous apelin-13 induces the expression of GFAP in retinal astrocytes.** (A–C) Effect of apelin-13 in WT mouse retina. (A) Retinas were stained with antibodies against PDGFR $\alpha$ , GFAP and PECAM1 at P5, 48 hours after intraocular injection with PBS or apelin-13. (B) qPCR analysis of *Gfap* using mRNA from FACS-sorted PDGFR $\alpha$ <sup>+</sup> cells of P5 retina (\*\* $P$ <0.01). (C) Capillary density behind the first vascular loop after injection with apelin in WT mouse retina ( $n$ =6). N.S., not significant. (D–F) Rescue of aberrant overgrowth of astrocytes observed in *Apln* KO mice by intraocular injection of apelin-13. (D) Retinas were immunostained for PDGFR $\alpha$ , PAX2 and PECAM1 at P5, 48 hours after intraocular injection of PBS or apelin-13. (E) Quantitative evaluation of PAX2<sup>+</sup> astrocytes. Six random FOV in the retina were examined ( $n$ =6, \*\* $P$ <0.01). (F) Apelin reduces the capillary density from the vascular front in *Apln* KO mice ( $n$ =6, \* $P$ <0.05). The yellow dashed lines (D) demarcate the area (the first vascular loop) for which vascular density was calculated (C,F). Error bars indicate s.d. Scale bars: 100  $\mu$ m.

resulting in aberrant EC network formation. Because LIF is upregulated upon stimulation of APJ by apelin in ECs, and because LIF is widely accepted as a maturation factor for astrocytes (Bonni et al., 1997; Mi et al., 2001), we injected LIF into *APJ* KO mice to assess whether maturation of astrocytes inhibits overgrowth of ECs as well as astrocytes. Intraocular injection of LIF into *APJ* KO mice at P3 resulted in a reduction of the number of PDGFR $\alpha$ <sup>+</sup> astrocytes and improved the formation of dense sheets of astrocytes (Fig. 7D). Moreover, weakly GFAP-positive astrocytes became strong GFAP expressors. Furthermore, staining with anti-PECAM1 antibody indicated that aberrant overgrowth of ECs was not induced. Quantitative evaluation of the number of astrocytes (confirmed by PAX2 staining) revealed that the hyperproliferation observed in the vascular area was reduced, but that LIF injection did not influence the number of astrocytes in the avascular area where no overgrowth had previously been observed (Fig. 7E). It is accepted that immature weakly GFAP-positive astrocytes induce proliferation of ECs but that this is gradually reduced as their level of GFAP expression increases (Kubota et al., 2008; West et al., 2005). This was suggested to be caused by the expression of VEGF in immature astrocytes. We assessed *Vegf* mRNA expression in retinal PDGFR $\alpha$ <sup>+</sup> astrocytes from *APJ* KO mice at P5. We found that LIF injection attenuated *Vegf* transcription (Fig. 7F), suggesting induction of astrocyte maturation.

## DISCUSSION

Using a model of retinal angiogenesis, we have identified a possible mechanism by which maturation of astrocytes is induced as angiogenesis is finalized and newly developed blood vessels are consolidated. This entails apelin stimulation of APJ in ECs and subsequent LIF production, which induces maturation of weakly to strongly GFAP-positive astrocytes, which then enter quiescence. Because weakly GFAP-positive astrocytes act as proangiogenic accessory cells for ECs by producing VEGF and proliferate vigorously in response to PDGFA produced by ganglion cells, when LIF production is decreased due to the lack of apelin or APJ, the resulting aberrant overgrowth of immature astrocytes induces hyperproliferation of ECs. We propose that apelin/APJ activation in ECs is a trigger for finalization of blood vessel formation, indirectly mediated by the induction of astrocyte maturation.

We previously reported that although APJ is not expressed on ECs in the steady state after birth, in adulthood ischemia induces transient APJ expression in ECs mediated by stimulation with VEGF (Kidoya et al., 2008). In the retina, from the onset of retinal angiogenesis in newborn mice, network-forming ECs also transiently express APJ, which is downregulated after the establishment of the retinal endothelial network at P12 (Saint-Geniez et al., 2003). It has been reported using ISH that apelin is produced in tip cells, which might then induce proliferation of the stalk cells migrating behind them (del Toro et al., 2010). Apelin is secreted as peptides of 13 or 36 amino

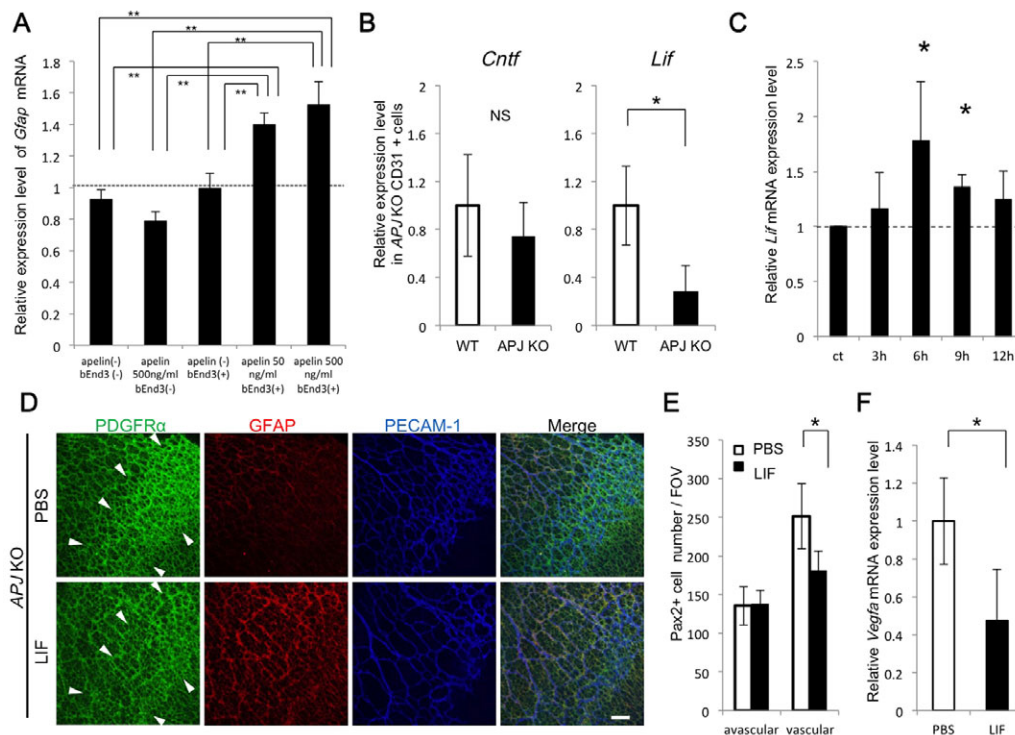


**Fig. 7. Overgrowth of immature astrocytes resulting from the lack of APJ in ECs is prevented by LIF.** (A) Effect on astrocyte GFAP positivity of medium conditioned by bEnd3 ECs stimulated with 50 ng/ml or 500 ng/ml apelin. Total RNA was extracted from dissociated retinal cells 24 hours after treatment with conditioned medium and qPCR analysis was performed to examine the expression of *Gfap* mRNA. \*\* $P < 0.01$ . (B) qPCR analysis of *Cntf* and *Lif* using RNA isolated from FACS-sorted PECAM1<sup>+</sup> ECs of P6 mouse retinas ( $n=4$ , \* $P < 0.05$ ; N.S., not significant). (C) qPCR analysis of *Lif* mRNA expression in HUVECs. Total RNA was extracted from HUVECs stimulated with 50 ng/ml apelin for 0–12 hours ( $n=3$ , \* $P < 0.05$ ). (D–F) Effects of LIF on aberrant outgrowth of ECs and astrocytes. (D) Retinas of P5 *APJ* KO mice were dissected 48 hours after intraocular injection of PBS or LIF and stained with antibodies against PDGFR $\alpha$ , GFAP and PECAM1. LIF inhibited astrocyte proliferation (surrounded by arrowheads) and induced upregulation of GFAP even ahead of the sprouting edge. Scale bar: 100  $\mu$ m. (E) Quantitative evaluation of the number of PAX2<sup>+</sup> astrocytes in vascular or avascular areas of *APJ* KO retina after treatment with PBS or LIF ( $n=3$ , \* $P < 0.05$ ). (F) qPCR analysis of *Vegfa* mRNA expression in sorted PDGFR $\alpha$ <sup>+</sup> cells of P5 PBS- or LIF-treated *APJ* KO retinas ( $n=3$ , \* $P < 0.05$ ). Error bars indicate s.d.

acids. It is possible that apelin affects ECs that are continuously expressing APJ in the retina, not only locally but also in a wider context. While apelin in the retina has been reported to have proangiogenic properties (del Toro et al., 2010), we previously reported that it also acts as a maturation factor for newly developing blood vessels. It induces the assembly of ECs, and thus promotes the formation of larger blood vessels (Kidoya et al., 2008). It also stabilizes the junction protein VE-cadherin and thus inhibits vascular hyperpermeability induced by VEGF or inflammatory stimuli (Kidoya et al., 2010). Therefore, diverse functions for apelin during angiogenesis have been postulated. VEGF has strong proangiogenic activity, but also induces the production of vasohibin 1, which has anti-angiogenic activity (Watanabe et al., 2004). This implies that proangiogenic factors might also concurrently induce anti-angiogenic factors in ECs as part of a negative-feedback regulatory mechanism. LIF production from ECs upon activation of APJ might also be involved in such a negative-feedback system during angiogenesis. Based on the phenotype of *Apln* KO or *APJ* KO mice, we conclude that apelin facilitates angiogenesis by inducing proliferation of ECs, but subsequently indirectly finalizes angiogenesis by furthering the maturation of astrocytes in the retina. Therefore, delay of capillary outgrowth from the optic nerve head, and the suppression of vascular network formation, are primarily defects induced by the lack of APJ or apelin. The partial hypervascularity subsequently observed in the migrating front of the vascular network-forming area is, indirectly, a secondary deficit caused by insufficient maturation of astrocytes.

We previously reported that TIE2 activation by ANG1 in ECs is one pathway of apelin production (Kidoya et al., 2008). Consistent with ANG1 regulating the enlargement of blood vessels, we found that apelin also induces enlarged blood vessels by promoting the assembly of ECs. Based on these findings, we reported apelin as a factor for constructing enlarged blood vessels and that it acts as a downstream regulator of the ANG1/TIE2 system. We initially focused on enlargement of blood vessels in retinas from *APJ* KO mice. However, *APJ* KO mice showed moderate defects of vascular network formation in their retinas and we could not clearly compare vascular diameters because of delayed blood vessel formation in these mice.

ANG1 production is usually induced in mural cells, which are located beside both tip cells and stalk cells. With respect to mural cell localization, WT and *APJ* KO mice were indistinguishable (supplementary material Fig. S4). Therefore, ANG1 might affect both tip cells and stalk cells. Because apelin mRNA is expressed predominantly in tip cells in the retina (del Toro et al., 2010; Strasser et al., 2010), these might possess a specific machinery for apelin production, which could be affected by ANG1. However, mechanisms regulating apelin production in tip cells have not been elucidated. It has previously been reported that ANG1 is produced by astrocytes upon re-oxygenation after ischemia and has been suggested to play an important role in the barrier function associated with tight junction proteins (Lee et al., 2003). We previously reported that apelin also induces stabilization of VE-cadherin in ECs, as

described above (Kidoya et al., 2010). Therefore, further studies of the relationship between ANG1 and apelin and of the additional involvement of other mechanisms regulating apelin production in tip cells as influenced by mural cells or astrocytes are required.

In the brain, neural precursor cells (NPCs) generate neurons and subsequently glia. This switch is crucial for determination of the number of neurons and glia. Mechanisms regulating the differentiation of glia from NPCs, such as how and where the commitment to the glial lineage is made, have been extensively analyzed (Freeman, 2010; Rowitch and Kriegstein, 2010). However, regulation of astrocyte differentiation from immature to mature cells in vivo is not well characterized. One line of evidence suggests that oxygen levels control astrocyte differentiation, i.e. inadequate vascularity in the retina induces hypoxia, resulting in the suppression of astrocyte differentiation (West et al., 2005). Reciprocally, well-organized vascular formation triggers maturation of astrocytes under normoxia. Deficiency of APJ also induces hypoxia because of insufficient outgrowth of blood vessels; such hypoxia may then induce hypervascularity caused by VEGF upregulation and release from immature astrocytes. It is possible that maturation arrest of astrocytes might be secondary to the lack of APJ; however, we found that expression of LIF, an astrocyte maturation factor, is induced in ECs by stimulation with apelin. Because LIF expression is reduced in *APJ* KO mice, these data suggest that complex mechanisms, such as hypoxia and attenuation of LIF, underlie the suppression of astrocyte maturation in *APJ* KO mice.

Although it has been reported that LIF secreted by ECs induces astrocyte maturation (Kubota et al., 2008; Mi et al., 2001), how LIF is induced in ECs in vivo has not been determined. Our present data suggest that LIF production mediated by activation of APJ in ECs by apelin is one of the programmed processes regulating maturation of astrocytes in vivo, which facilitates well-organized vascular and astrocyte network formation in the retina. However, it has been reported that *Lif* KO mice show overall hypervascularity in their retinas (Kubota et al., 2008) and this phenotype is different from that of *APJ* KO mice because hypervascularity was restricted to the migrating front of the vascular network area in these latter mice. GFAP positivity in astrocytes at areas other than the migrating front of the vascular network did not differ between WT and *APJ* KO mice (Fig. 2A). This suggests the existence of mechanisms other than the apelin/APJ system for astrocyte maturation and indicates that further investigation is required to achieve a full understanding of the molecular mechanisms of blood vessel and astrocyte maturation.

#### Acknowledgements

Special thanks are due to Yoshiaki Kubota (Department of Cell Differentiation, Sakaguchi Laboratory, School of Medicine, Keio University, Shinjuku-ku, Tokyo, Japan) for outstanding technical support. We also thank Ping Xie for technical support and Keisho Fukuhara and Noriko Fujimoto for general assistance.

#### Funding

This work was partly supported by a grant from the Ministry of Education, Science, Sports, and Culture of Japan.

#### Competing interests statement

The authors declare no competing financial interests.

#### Supplementary material

Supplementary material available online at <http://dev.biologists.org/lookup/suppl/doi:10.1242/dev.072330/-DC1>

#### References

Augustin, H. G., Koh, G. Y., Thurston, G. and Alitalo, K. (2009). Control of vascular morphogenesis and homeostasis through the angiopoietin-Tie system. *Nat. Rev. Mol. Cell Biol.* **10**, 165-177.

- Bonni, A., Sun, Y., Nadal-Vicens, M., Bhatt, A., Frank, D. A., Rozovsky, I., Stahl, N., Yancopoulos, G. D. and Greenberg, M. E. (1997). Regulation of gliogenesis in the central nervous system by the JAK-STAT signaling pathway. *Science* **278**, 477-483.
- Chu, Y., Hughes, S. and Chan-Ling, T. (2001). Differentiation and migration of astrocyte precursor cells and astrocytes in human fetal retina: relevance to optic nerve coloboma. *FASEB J.* **15**, 2013-2015.
- del Toro, R., Prahst, C., Mathivet, T., Siegfried, G., Kaminker, J. S., Larrivee, B., Breant, C., Duarte, A., Takakura, N., Fukamizu, A. et al. (2010). Identification and functional analysis of endothelial tip cell-enriched genes. *Blood* **116**, 4025-4033.
- Freeman, M. R. (2010). Specification and morphogenesis of astrocytes. *Science* **330**, 774-778.
- Fruttiger, M., Calver, A. R., Kruger, W. H., Mudhar, H. S., Michalovich, D., Takakura, N., Nishikawa, S. and Richardson, W. D. (1996). PDGF mediates a neuron-astrocyte interaction in the developing retina. *Neuron* **17**, 1117-1131.
- Gariano, R. F. (2003). Cellular mechanisms in retinal vascular development. *Prog. Retin. Eye Res.* **22**, 295-306.
- Gerhardt, H., Golding, M., Fruttiger, M., Ruhrberg, C., Lundkvist, A., Abramsson, A., Jeltsch, M., Mitchell, C., Alitalo, K., Shima, D. et al. (2003). VEGF guides angiogenic sprouting utilizing endothelial tip cell filopodia. *J. Cell Biol.* **161**, 1163-1177.
- Ishida, J., Hashimoto, T., Hashimoto, Y., Nishiwaki, S., Iguchi, T., Harada, S., Sugaya, T., Matsuzaki, H., Yamamoto, R., Shiota, N. et al. (2004). Regulatory roles for APJ, a seven-transmembrane receptor related to angiotensin-type 1 receptor in blood pressure in vivo. *J. Biol. Chem.* **279**, 26274-26279.
- Kasai, A., Shintani, N., Kato, H., Matsuda, S., Gomi, F., Haba, R., Hashimoto, H., Kakuda, M., Tano, Y. and Baba, A. (2008). Retardation of retinal vascular development in apelin-deficient mice. *Arterioscler. Thromb. Vasc. Biol.* **28**, 1717-1722.
- Kidoya, H., Ueno, M., Yamada, Y., Mochizuki, N., Nakata, M., Yano, T., Fujii, R. and Takakura, N. (2008). Spatial and temporal role of the apelin/APJ system in the caliber size regulation of blood vessels during angiogenesis. *EMBO J.* **27**, 522-534.
- Kidoya, H., Naito, H. and Takakura, N. (2010). Apelin induces enlarged and nonleaky blood vessels for functional recovery from ischemia. *Blood* **115**, 3166-3174.
- Kishimoto, T., Akira, S., Narazaki, M. and Taga, T. (1995). Interleukin-6 family of cytokines and gp130. *Blood* **86**, 1243-1254.
- Kubota, Y., Hirashima, M., Kishi, K., Stewart, C. L. and Suda, T. (2008). Leukemia inhibitory factor regulates microvessel density by modulating oxygen-dependent VEGF expression in mice. *J. Clin. Invest.* **118**, 2393-2403.
- Kurihara, T., Kubota, Y., Ozawa, Y., Takubo, K., Noda, K., Simon, M. C., Johnson, R. S., Suematsu, M., Tsubota, K., Ishida, S. et al. (2010). von Hippel-Lindau protein regulates transition from the fetal to the adult circulatory system in retina. *Development* **137**, 1563-1571.
- Lee, S. W., Kim, W. J., Choi, Y. K., Song, H. S., Son, M. J., Gelman, I. H., Kim, Y. J. and Kim, K. W. (2003). SSeCKS regulates angiogenesis and tight junction formation in blood-brain barrier. *Nat. Med.* **9**, 900-906.
- Mi, H., Haerberle, H. and Barres, B. A. (2001). Induction of astrocyte differentiation by endothelial cells. *J. Neurosci.* **21**, 1538-1547.
- Rowitch, D. H. and Kriegstein, A. R. (2010). Developmental genetics of vertebrate glial-cell specification. *Nature* **468**, 214-222.
- Saint-Geniez, M., Argence, C. B., Knibiehler, B. and Audigier, Y. (2003). The *mnr/apj* gene encoding the apelin receptor is an early and specific marker of the venous phenotype in the retinal vasculature. *Gene Expr. Patterns* **3**, 467-472.
- Sato, T. N., Tozawa, Y., Deutsch, U., Wolburg-Buchholz, K., Fujiwara, Y., Gendron-Maguire, M., Gridley, T., Wolburg, H., Risau, W. and Qin, Y. (1995). Distinct roles of the receptor tyrosine kinases Tie-1 and Tie-2 in blood vessel formation. *Nature* **376**, 70-74.
- Strasser, G. A., Kaminker, J. S. and Tessier-Lavigne, M. (2010). Microarray analysis of retinal endothelial tip cells identifies CXCR4 as a mediator of tip cell morphology and branching. *Blood* **115**, 5102-5110.
- Suri, C., Jones, P. F., Patan, S., Bartunkova, S., Maisonpierre, P. C., Davis, S., Sato, T. N. and Yancopoulos, G. D. (1996). Requisite role of angiopoietin-1, a ligand for the TIE2 receptor, during embryonic angiogenesis. *Cell* **87**, 1171-1180.
- Takakura, N., Watanabe, T., Suenobu, S., Yamada, Y., Noda, T., Ito, Y., Satake, M. and Suda, T. (2000). A role for hematopoietic stem cells in promoting angiogenesis. *Cell* **102**, 199-209.
- Uemura, A., Kusuhara, S., Wiegand, S. J., Yu, R. T. and Nishikawa, S. (2006). Tlx acts as a proangiogenic switch by regulating extracellular assembly of fibronectin matrices in retinal astrocytes. *J. Clin. Invest.* **116**, 369-377.
- Watanabe, K., Hasegawa, Y., Yamashita, H., Shimizu, K., Ding, Y., Abe, M., Ohta, H., Imagawa, K., Hojo, K., Maki, H. et al. (2004). Vasohibin as an endothelium-derived negative feedback regulator of angiogenesis. *J. Clin. Invest.* **114**, 898-907.
- West, H., Richardson, W. D. and Fruttiger, M. (2005). Stabilization of the retinal vascular network by reciprocal feedback between blood vessels and astrocytes. *Development* **132**, 1855-1862.
- Zhang, Y. and Stone, J. (1997). Role of astrocytes in the control of developing retinal vessels. *Invest. Ophthalmol. Vis. Sci.* **38**, 1653-1666.

**Table S1. PCR primers**

Gene	Sequence (5' to 3')
Mouse <i>Gfap</i>	GCACTCAATACGAGGCAGTG GGCGATAGTCGTTAGCTTCG
Mouse vimentin	GAAATTGCAGGAGGAGATGC TCCACTTTCCGTTCAAGGTC
Mouse <i>Pax2</i>	CAAAGTTCAGCAGCCTTTCC GTTAGAGGCGCTGGAAACAG
Mouse <i>S100b</i>	GCACAAGCTGAAGAAGTCAGAA GAACTCCTGGAAGTCACACTCC
Mouse <i>Hif1a</i>	TCAAGTCAGCAACGTGGAAG TATCGAGGCTGTGTCGACTG
Mouse <i>Pdgfa</i>	ATTAACCATGTGCCCGAGAA TCTTGCAAACCTGCAGGAATG
Mouse <i>Vegfa</i>	AGCCGAGCTCATGGACGGGT AGTAGCTTCGCTGGTAGACATC
Mouse <i>Il6</i>	CACATGTTCTCTGGGAAATCG TCCAGTTTGGTAGCATCCATC
Mouse <i>Cntf</i>	AGCCTTGA CT CAGTGGATGG TGGAGGTTCTCTTGGAGTCG
Mouse <i>Lif</i>	AACTGGCACAGCTCAATGG AGGCGCACATAGCTTTTCC
Mouse oncostatin M	CAGAATCAGGCGAACCTCAC TCAGGTCAGGTGTGTTTCAGG
Mouse <i>Il11</i>	CTGGGACATTGGGATCTTTG TGGCTCCAGAGTCTTTAGGG
Mouse cardiotrophin 1	ACCACCAGACTGACTCCTCAA CTGCACGTATTCTCCAGAAG
Mouse <i>Gapdh</i>	TGGCAAAGTGGAGATTGTTGCC AAGATGGTGATGGGCTTCCCG
Human <i>LIF</i>	CACAACAACCTCATGAACCAG CCACATAGCTTGTCCAGGTTG
Human <i>GAPDH</i>	GAAGGTGAAGGTCGGAGTC GAAGATGGTGATGGGATTTC